IMPROVED LANDSMAN CONVERTER FOR PV BASED AGRICULTURE MOTOR PUMP SYSTEM

Abstract

For large-scale water pumping applications including farm irrigation and water for drinking delivery, electrical pumps are frequently employed. But locations that are not linked to the public electrical distribution network cannot use electric pumps. Such remote locations require the use of electric pumps powered by RES like solar energy systems. Consequently, in recent years, interest in solar-powered water pumping devices has surged. It is suggested to use an upgraded Landsman converter supplied BLDC motor in a solar-powered water pumping system. It offers a water pumping system powered by PV that is functional and economical. The BLDC is switched using an upgraded Landsman converter with lower cost and volume. The water pump is further driven by a BLDC motor, which is connected to a 3ØVSI, which transforms the DC voltage to its corresponding AC voltage. In order to increase the PV output power and maintain it at its maximum under variable irradiance, a modified P&O MPPT controller is employed. Between a solar energy system and a motor-pump drive, an improved Landsman converter functions as a DC to DC converter where it achieve a voltage gain of 1:12 and efficiency of 97.42%. MATLAB Simulink model is used for simulating the entire system.

Keywords: Motor pump system, Improved DC-DC landsman converter, PV, Modified P&O MPPT controller, BLDC motor.

Authors

C. Fabbina
Research Scholar
Department of Electrical and Electronics Engineering
Government College of Engineering
Tirunelveli, Tamil Nadu, India.
fabbina2018@yahoo.com

P. Kavitha
Research Scholar
Department of Electrical and Electronics Engineering
Government College of Engineering
Tirunelveli, Tamil Nadu, India.
kavitha.paulsamy6@gmail.com

K. S. Kavin
Research Scholar
Department of Electrical and Electronics Engineering
Government College of Engineering
Tirunelveli, Tamil Nadu, India.
kavinksk@gmail.com

K. Sakthidhasan
Assistant Professor
Department of Electrical and Electronics Engineering
Vel Tech Multi Tech Dr. Rangarajan
Dr. Sakunthala Engineering College
India.
sakthidhasan@veltechmultitech.org

I. INTRODUCTION

Water pumping applications frequently employ electric pumps. But locations that are not linked to the public power grid are unable to utilise electric pumps for water pumping [1]. Such remote locations require the use of electric pumps powered by RES like solar energy systems. Therefore, in recent years, interest in solar-powered water pumping devices has surged. Uses for water pumping may involve moving water over substantial distances for things like agriculture irrigation, industrial water supply, water for drinking supply, fire prevention, treatment with bacteria, swimming pools, and waterfalls [2].

Due to the many benefits it offers over other options, solar energy has become one of the most popular energy sources today. There is no pollution associated with solar energy, and no greenhouse gas emissions occur. Additionally, it leads in less reliance on foreign oil and fossil fuels. Nearly the entire year may be powered by green and healthy solar energy. Solar panels require a lot of service during their lifetime. In overall, a system for pumping water is made up of a power source, a generator, and a water pump [3]. A solar PV array serves as the energy source in a solar-powered system. The solar generator's power is maximised by using the MPPT technology. Among the solar photovoltaic cell and the generator, a Landsman converter serves as the power filtering phase. The MPPT approach used is called the incremental conductance (IC) algorithm [4]. It produces the ideal duty ratio for the Landsman converter's switches. Induction motors were traditionally utilised for applications involving the pumping of water. However, using this controller came with difficulties, including inadequate performance, ineffectiveness, and complicated control [4, 5]. Because it is straightforward, the Perturb and Observe MPPT approach is used. Applications involving water pumping using DC machines were also examined. However, their use was constrained by the need for frequent maintenance and breakdowns brought on by the existence of commutator and brushes. Researchers were briefly drawn to using Permanent Magnet Synchronous Motors because of their great efficiency and little maintenance needs [6]. Although PMSM is becoming more popular due to its superior power density and effectiveness, it remains unfeasible to substitute an induction motor since this is the most durable and affordable motor [7]. The difficulties associated with employing ferrite magnets in a high-power rotor surface magnet depending PMSM stay in spite of the modelling and creation of low cost PMSM employing low cost ferrite magnets as opposed to rare-earth ones due to their less powerful magnetic characteristics contrasted to the rare-earth magnets and the potential danger of permanent demagnetization [8–9]. However the system was pricey because of the inclusion of permanent magnets.

The switching type generators that are utilised most frequently are boost converters because the voltage that they generate will be higher than the matching input voltage. Its improved dynamic responsiveness has led to its widespread implementation in solar power systems. The Landsman converter is a high-tech DC-DC converter that can adjust power factor, maintain a steady output voltage, eliminate distortion caused by harmonics, and manage DC voltage in a single stage using just one control method. When contrasted to other converters like the Zeta, CUK, and SEPIC, the Landsman converter uses a fraction of the passive parts [10–13]. In contrast to LUO converters and canonical switching cell (CSC) converters, it does not call for a particular input ripple filter. When compared with previous buck-boost converters like the CUK converter, the input inductor employed in the proposed Landsman converter is rather modest. One of the Landsman converter's finest qualities is that

it functions as a DC-DC boost converter to generate a smooth temporary response. Other benefits include improved dynamic output voltage, reduced ripple content, and a quick settling time. Therefore, closed loop voltage and current controllers are taken into consideration to produce the optimum response to transients and excellent dynamic voltage [14, 15]. In spite of increasing the voltage gain, improved Landsman converters are employed in purposes like tracking the maximum power from PV arrays.

This research acts as a guide for professionals who want to learn about PV-fed pumps and aids with comprehending the negative impact that partial shade may have on the complete WPS if the circumstances are ignored. Due to its unique technological impact on the area of water pumping systems, this research provides a comprehensive foundation for technical elements of BLDC-based water pumping systems. For the best use of the solar PV array, a modified P&O-based MPPT approach is used. The structure of the essay is as following. Some of the overview of relevant studies is provided in Section II. The suggested system's system structure and models are discussed in Section III. Sections IV and V examine the study's findings and the result.

II. RELATED WORKS

1. **Arjun M et al [2018]** [16] have made a work which includes a simulation- and experiment-based examination of the impact of partial shade situations on pumps. The findings of the model and the experiment are discovered to be in strong agreement. Therefore, this study's effort aids in comprehending the negative impacts brought on by partial shading situations and serves as a resource for professionals who desire to learn about PV fed pumps. It continues to receive uniform illumination, and further research is necessary.

2. **Saurabh Shukla et al [2018]** [17] have studied to build, manage, and put into practise a PV array fed speed sensorless DTC of an IM drive for water pumping in both independent and battery-connected hybrid modes. Speed prediction uses the stator flux calculated by the suggested flux observer. Because of the system's advantages of simplicity, control, cost-effectiveness, somewhat excellent effectiveness, and small size, it is assumed that its applicability may be assessed by placing it in the field.

3. **Mohamed N. Ibrahim et al [2019]** [18] have made a study under situations of partial shade, it is suggested that a PV pumping system with a SRM function better. The DC-DC converter, which is primarily utilised to raise the PV array's power output, is not part of the entire system. Batteries for storage are also not contained, in additional. The SRM is driven by a normal inverter that is linked straight to the PV array. Additionally, a control method is suggested for operating the inverter so that the PV array's highest power output is attained while the SRM is operating at the highest torque. As a consequence, the effectiveness and cost of the system are increased.

4. **Bhim Singh et al [2018]** [19] have discussed an effective way to deliver a field-oriented controlled PMSM drive to a WPS using a solar PV array and 1∅ grid. Because of the erratic operation of PV systems, a single system is unable to meet the demand for a reliable water supply. A grid intergraded WPS is suggested here as a way to lessen this.

Due to the restrictions of the testing facility, the water pump's feature is achieved using an independently stimulated DC generator.

5. **K. K. Prabhakaran et al [2020]** [20] have presented a standalone PV supplied PMSM drive for pumping water is suggested. By utilising a reduced switch inverter (RSI), the suggested solution seeks to lower switching losses and overall costs. The suggested system consists of a PMSM drive that is powered by a PV source through an inverter with fewer switches than usual. The standard VSI requires six switches, but the inverter only needs four. The PMSM drive is managed via a field-oriented control system. The speed reference for the PMSM drive is produced using P&O MPPT approach.

III. PROPOSED SYSTEM

In this paper, a BLDC motor drive with a 3VSI foundation is suggested for use in water pumping applications. The suggested system consists of a BLDC motor that is powered by a PV source through a converter and an inverter with fewer switches than usual. In addition to increased pumping system dependability, this makes it feasible to utilise a PV array and motor pump to their maximum potential.

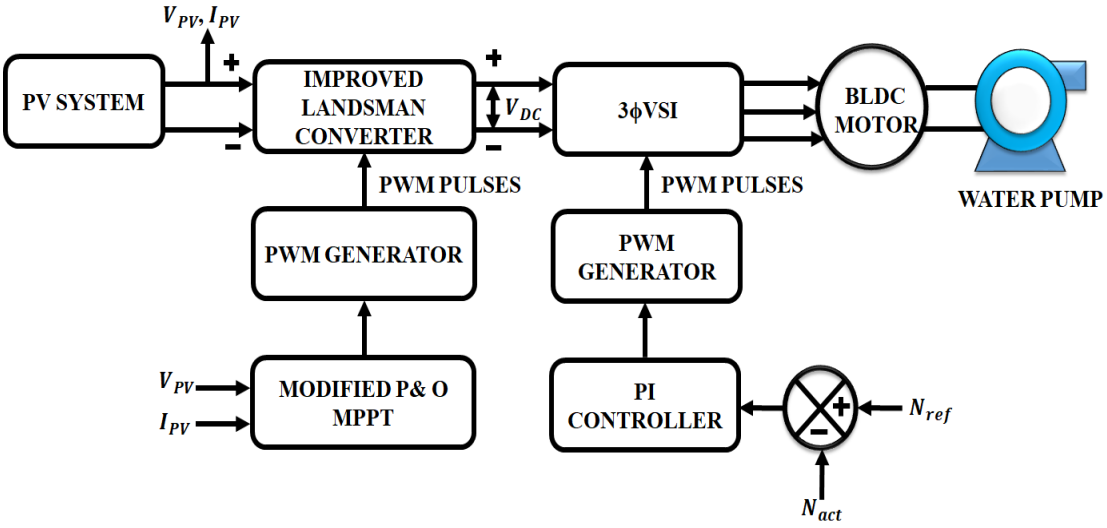

Figure 1: Proposed System

The suggested BLDC motor-WPS based on a PV energy conversion system is shown in Figure 1. Here, enhanced Landsman converters are employed to capture solar energy with a high gain. In photovoltaic systems, it has the ability to step up the voltage from a low level to a high level. The VSI that feeds the BLDC motor-pump has a direct connection to the DC-DC converter. Because the rotor has no windings, it is not susceptible to centrifugal forces. Additionally, because the windings are supported by the housing, they may be cooled by conduction without the need for airflow inside the motor. For the best use of the solar PV array, a P&O-based MPPT approach is used. Utilising PV voltage and current as input signals, this technique generates an ideal duty ratio corresponding to the maximum output of a solar PV array. The solar panel is connected to a three-phase electrical network via the PI controller, which is utilised to regulate the three-phase inverter.

1. **Solar Pv System:** The solar PV module was created to operate at 15 KW with a constant solar irradiation of 1000W/m2 and a temperature of 25°C. There are other methods to build the simplified circuit of a solar PV cell, but the single-diode model is the one that is widely used since it is simple to create, less complicated, and more accurate. The single-diode architecture of a solar PV cell was used to construct a solar PV module. The single diode model's I-V relation is controlled by:

$$I = I_{ph} - I_o \left\{ e^{\frac{q(V+R_s I)}{AKT}} - 1 \right) - \frac{V+R_s I}{R_{sh}} \quad (1)$$

where I_o is the diode saturating current, R_{sh} is the shunt resistance, and I_{ph} is the photocurrent of the diode. The Boltzmann constant (1.38x1023J/K), series resistance (R_s), the factor of ideality (A), the charge of an electron (q).

2. **Design of Improved Landsman Converter:** In order to lessen the current and voltage strain on the electrically powered semiconductor device, the improved Landsman converter is built to run in CCM. Figure 2 depicts a schematic for the improved Landsman DC-DC Converter. Its functioning can be examined by taking into account the two modes indicated, and the appropriate modes of operation waveforms may be produced.

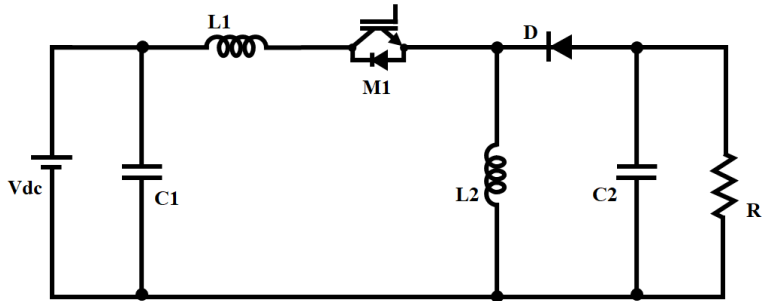

Figure 2: Circuit Diagram of Improved Landsman Converter

3. **Mode 1- when switch is ON:** The circuit design in Figure 3 is the consequence of the voltage across intermediary capacitor C_1 that reverse biassed the diode when the switch is in the ON position VC_1 . As the output voltage V_0 is greater than the inductor current I_L, which is flowing through a closed switch, VC_1 discharges via the switch, delivering energy to the inductor L and the output. As a consequence, as seen in Figure 3, VC_1 declines and I_L rises. Energy is delivered by the input to input inductor L_1.

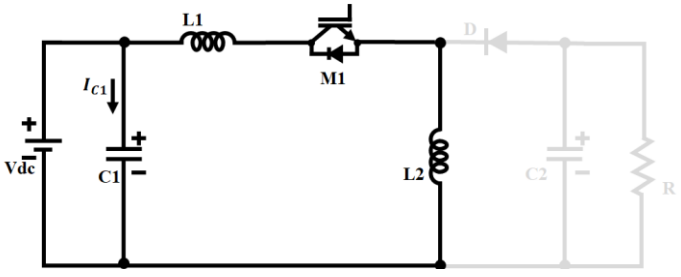

Figure 3: Mode I operation

4. **Mode 2- when switch is OFF:** The diode flows when the switch is in the "OFF" position because it is now forward biassed, creating the circuit design shown in Figure 4. The energy retained in Mode I has been converted to output across the diode as the inductor current I_L now passes through it. Alternately, energy from both the input and L_1 is being used to charge C_1 through the diode. It has the effect of making VC_1 rise and IL fall, as seen in Mode II's Figure 4.

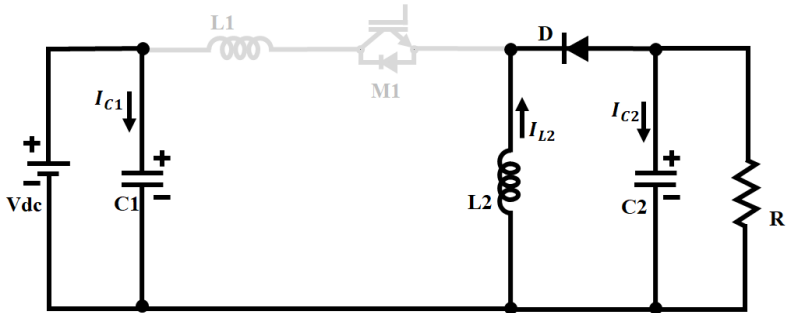

Figure 4: Mode II Operation

By taking into account the waveform as illustrated in Figure 5, it is possible to compute the ripple content contained in the input current that travels through L_1 . Let's suppose that C_1 receives all of the ripple component of L_1 current during CCM operation. An extra flux is represented by the darkened region in the waveform of VC_1 .

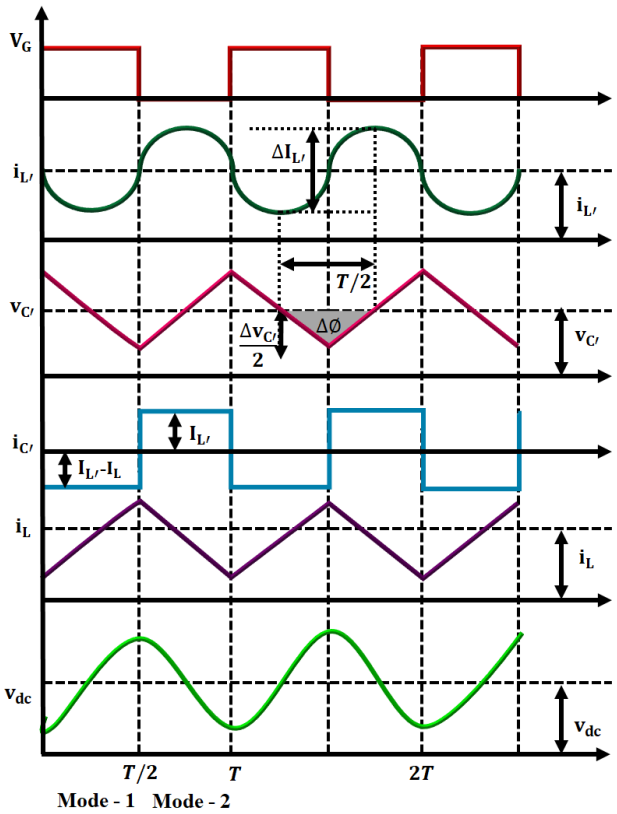

Figure 5: Waveforms of improved Landsman Converter

As a result, the peak to peak current ripple passing through L_1may be expressed as

$$\Delta IL_1 = \frac{\Delta \emptyset}{L_1} = \frac{1}{L_1}\frac{1}{2}\frac{\Delta VC_1}{2}\frac{T}{2} \quad (2)$$

The current via C_1 is denoted in Mode II function as

$$iC_1 = IL_1 = C_1 \frac{\Delta VC_1}{(1-D)T} \quad (3)$$

where T stands for the switching time period and D stands for the duty cycle ratio. Using equation (3), the voltage ripple content in ΔVC_1 is calculated as follows:

$$\Delta VC_1 = \frac{IL_1}{C_1}(1-D)T \quad (4)$$

Consequently, adding ΔVC_1 from equation (4) to equation (2) results in

$$\Delta IL_1 = \frac{1}{L_1}\frac{1}{2}\frac{IL_1}{2C_1}(1-D)T\frac{T}{2} \quad (5)$$

$$\Delta IL_1 = \frac{1}{8L_1C_1}\ \frac{IL_1(1-D)}{f_{sw}^2} \quad (6)$$

The above can be normalized as,

$$\frac{\Delta IL_1}{IL_1} = \frac{1}{8L_1C_1}\ \frac{(1-D)}{f_{sw}^2} \quad (7)$$

where the switching frequency is given by f_{sw}^2 = 1/T. The link between input and output makes it clear that

$$IL_1 = \frac{D}{1-D} I_{dc} \quad (8)$$

where I_{dc} is the Landsman converter's output current. As a result, by rearranging the variables and putting IL1 from equation (6) into equation (4), we arrive at

$$L_1 = \frac{DI_{dc}}{8f_{sw}^2 \Delta IL_1 C_1} \quad (9)$$

Dc-dc converters have typically been controlled using linear voltage mode and current mode techniques. These types of controllers perform better with small signals at the desired point of operation due to characteristics including consistent switching frequency ranges, zero error in steady-state, and higher small-signal effectiveness.

5. **P&O based MPPT Algorithm:** A solar PV module should run at MPP in order to generate the most electricity possible, as shown in Figure 6 (A). Operating at MPP aids in overcoming the primary disadvantage of PV systems, which is their poor conversion effectiveness, which ranges from 7 to 19%. Different MPPT methods have been researched thus far, and they not only track MPP but also determine the DC link voltage

by correctly and effectively controlling the converter. The most popular MPPT method and one that is based on V_{PV} perturbation is P&O.

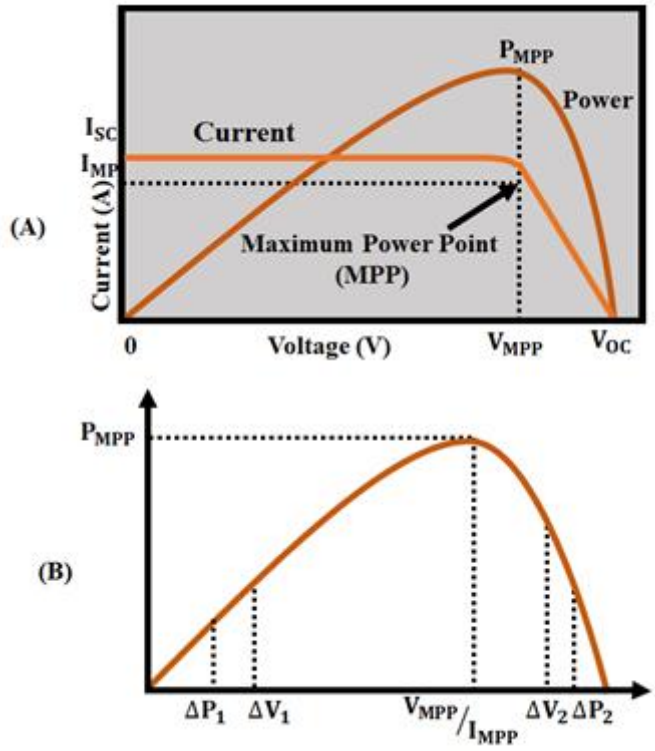

Figure 6: (A) Voltage and Current at MPP (B) The solar system's P-V Curve

As observed in Figure 6(B), moving up the slope on the left side of the P-V curve increases the operating point towards MPP, whilst moving down the slope on the right side shifts the operating point away from MPP. As a result, the controlled variable V_{PV} of the MPPT may be expressed as follows:

$$V_{PV,new} = V_{PV,old} + \Delta V_{PV} \times \beta \quad (10)$$

where PV is the perturbations step size and the track vector is indicated by the multiplier. Upto MPP, the opposite direction of the multiplier is kept constant. When the MPP has been reached and raised, the power begins to decrease, which changes its polarity and pushes the point of operation towards the MPP from the other direction of the curve, causing the operating point to begin to oscillate about the MPP. By reducing the step size, the motion can be stopped, but at the expense of the system's dynamic responsiveness. P&O technique has been widely utilised because it is accurate, simple, and feasible, but because MPPT effectiveness is determined by the perturbation step size, there is a trade-off between effectiveness and speed of convergence.

6. **Modelling of Bldc Motor:** A BLDC motor's modelling may be created in a similar way as a 3∅ synchronous machine. Some dynamic properties are altered since the rotor has a permanent magnet installed on it. The substance of the magnet affects the flux linkage from the rotor. Consequently, magnetic flux linkage saturation is typical of these type of

motors. One construction of the BLDC motor flows by a three-phase voltage source, like any normal three-phase motor. It's not required that the source be sinusoidal. As soon as the peak voltage is under the maximum voltage limitation of the motor, any wave shape, including square waves, may be used. Similarly to that, the BLDC motor's armature winding model is expressed as follows,

$$V_a = Ri_a + L\frac{di_a}{dt} + e_a \quad (11)$$

$$V_b = Ri_b + L\frac{di_b}{dt} + e_b \quad (12)$$

$$V_c = Ri_c + L\frac{di_c}{dt} + e_c \quad (13)$$

$$e_a = K_w f(\theta_e)\omega \quad (14)$$

$$e_b = K_w f(\theta_e - 2\pi/3)\omega \quad (15)$$

$$e_c = K_w f(\theta_e + 2\pi/3)\omega \quad (16)$$

$$\theta_e = \frac{P}{2}\theta_m \quad (17)$$

The total of the torque outputs from each phase may be used to indicate the overall torque. The following equation shows the overall torque output:

$$T_e = \frac{e_a i_a + e_b i_b + e_c i_c}{\omega} \quad (18)$$

Where T_e is the total torque produced (in Nm). This is how the equation for a mechanical part is represented.

$$T_e - T_l = J\frac{d\omega}{dt} + B\omega \quad (19)$$

The greatest power from the solar PV array that is readily accessible controls the speed. Any fluctuation in the atmosphere affects the power output of the PV array, which affects the speed of the BLDC motor.

IV. RESULT AND DISCUSSIONS

Utilising the MATLAB/ SIMULINK environment, a model for simulation for the PV system using three phase VSI is being successfully constructed. A constant irradiation of 1000 W/m^2 is used to assess the efficiency of the PV. The PV voltage, PV current, and maximum power output of the PV array are the outcome metrics taken into account for the assessment. Table 1 provides the parameter specifications for PV and the upgraded landsman converter.

Table 1: Parameter Specifications

Parameters	**Rating**
PV system	
Peak power	10 KW
Capacity	$5W$
Number of panels	20
Improved Landsman converter	
L_1, L_2	1 mH
C_1,C_2	4.7 μF

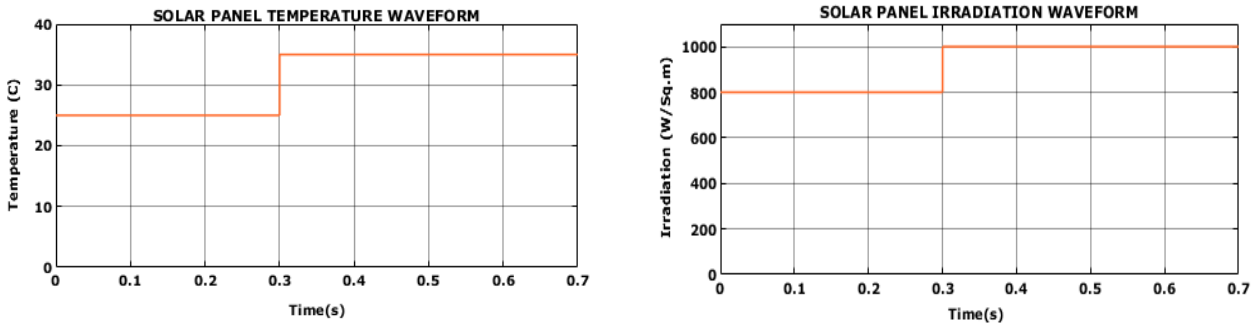

(a) (b)

Figure 7: PV waveform (a) Temperature (b) Irradiance

The model for simulation was created with a constant temperature of 25 °C in mind, and all voltage and current calculations have been completed.

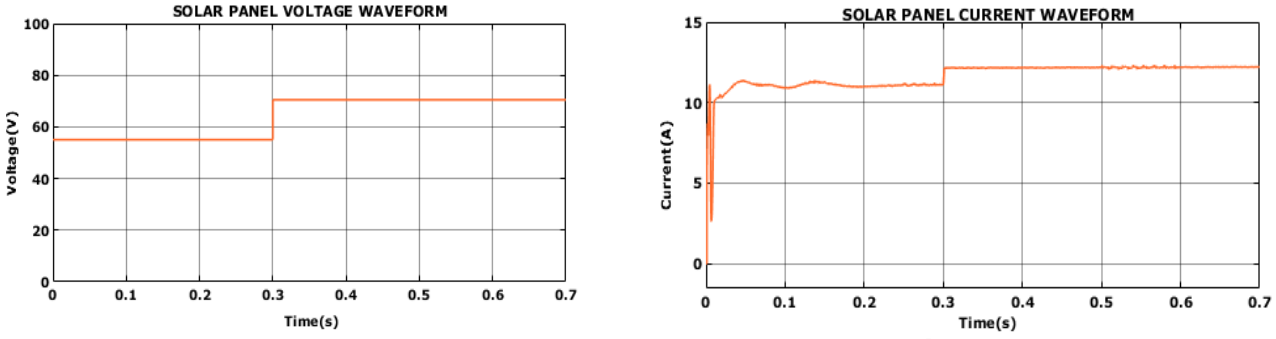

(a) (b)

Figure 8: PV waveform (a) Voltage (b) Current

The output DC voltage and current of the PV array are depicted in figures 7 (a) and (b), accordingly. According to the modelling data that was collected, the V_{PV} and I_{PV} that were produced represent the PV array voltage and are 70 V and 12 A, correspondingly.

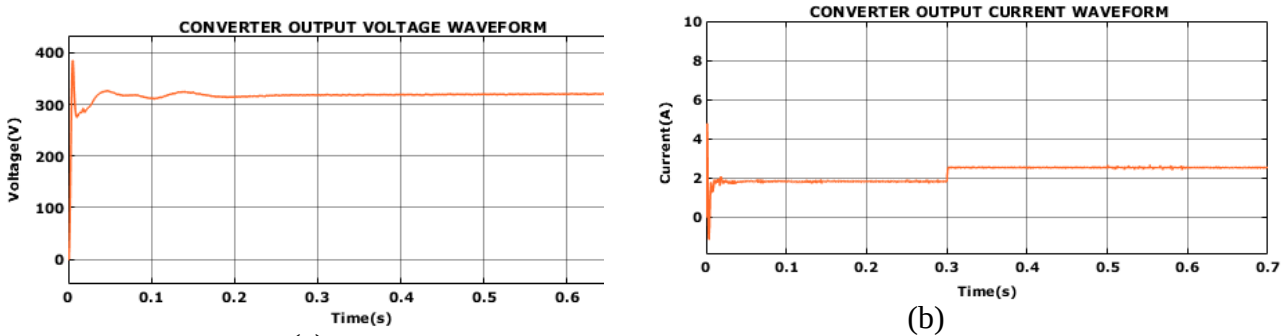

(a) (b)

Figure 9: Output Voltage (a) and Current (b) of Proposed Converter

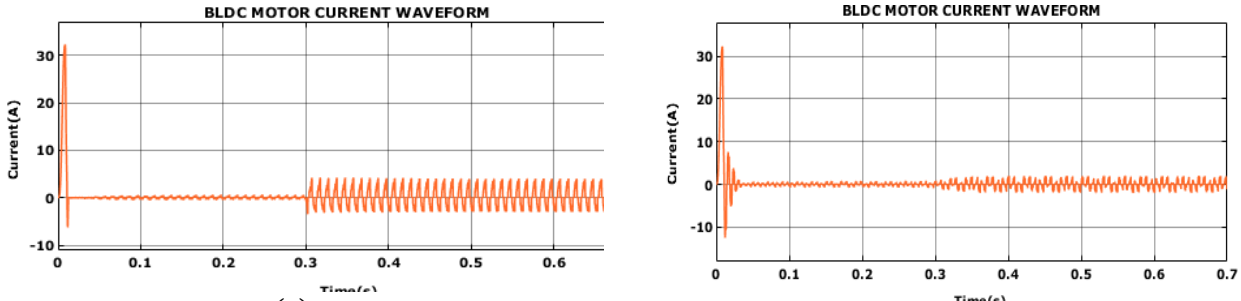

(a) (b)

Figure 10: BLDC motor current (a) 1500 RPM (b) 2500 RPM

The three phase currents of a BLDC motor are depicted in Figure 10. When the speed reaches a stable value, the initial current is large, but it soon drops to the rated value.

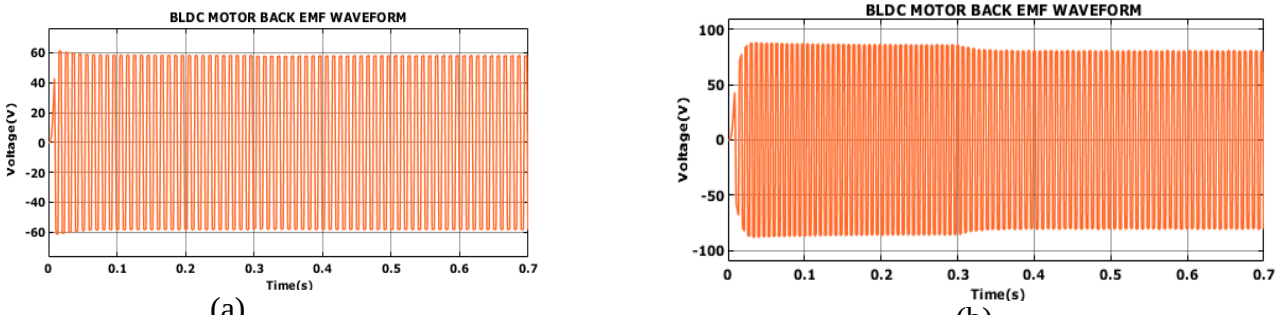

(a) (b)

Figure 11: BLDC motor back emf (a) 1500 RPM (b) 2500 RPM

The trapezoidal back emf wave shape is seen in Figure 11. We have thought about the 120-degree manner of operation here.

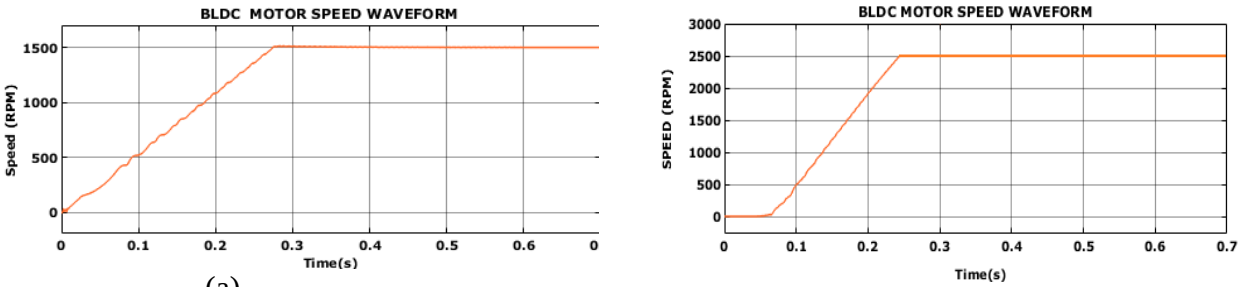

(a) (b)

Figure 12: BLDC motor Speed (a) 1500 RPM (b) 2500 RPM

Figure 12 depicts the motor's speed under PI control. When using PI control, the motor quickly approaches the reference speed, which in this case is 12000 rpm. At time t = 0.01 sec, the load torque increases from 0.28 Nm. At 2500 rpm, the load torque increases from 0.25 Nm

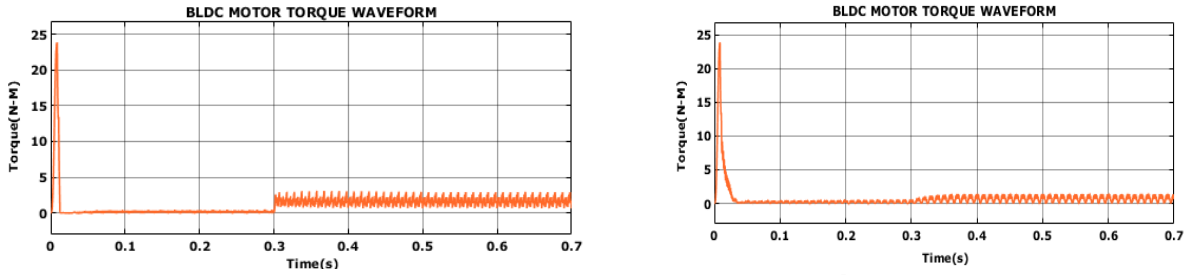

(a) (b)

Figure 13: BLDC motor torque (a) 1500 RPM (b) 2500 RPM

The motor's electromagnetic torque is seen in Figure 13. When the speed achieves a stable value, the initial torque is large, and it gradually reduces to the specified amount. When the load torque doubles at time t = 0.01 seconds, the electromagnetic torque likewise doubles by the same amount.

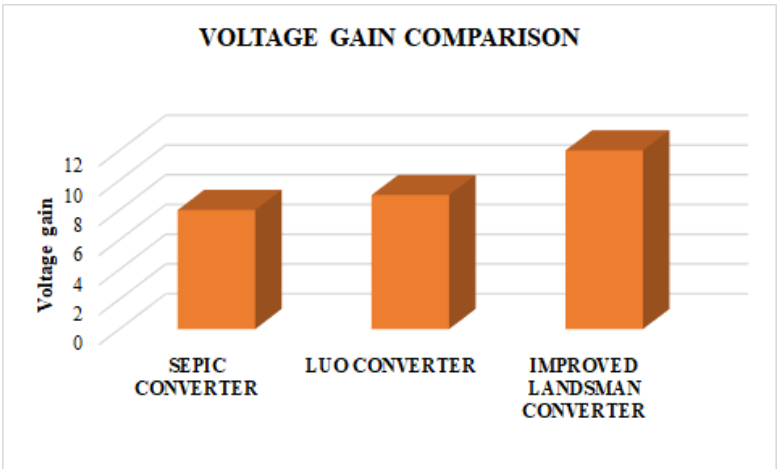

Figure 14: Comparison of voltage gain

A voltage gain analysis of the proposed I-Luo converter design in comparison to traditional converters is shown in Figure 14. Studies showed that the suggested converter increased voltage gain by 1:12 as claimed.

Table 2: Comparison of Converter Performance

Converters	**Voltage gain**	**Efficiency (%)**
SEPIC	1:8	88.82 % [21]
Luo	1:9	90% [22]
Improved Landsman	1:12	97.42%

The results of comparing the effectiveness of the suggested converter with that of traditional SEPIC and Luo converters are shown in Table 2. It has been determined that the suggested Improved Landsman converter design performs better than SEPIC and Luo converter architecture in terms of 97.42% efficiency and 1:12 voltage gain. According to this information, the PV system can efficiently raise the low DC voltage produced by the solar panels to an ideal voltage level that is suitable for grid integration.

V. CONCLUSION

Remote locations require the use of electric pumps powered by RES like solar energy systems. Consequently, in recent years, interest in solar-powered water pumping devices has surged. The analysis of a solar-powered BLDC drive for use in water pumping is studied in this paper. An upgraded Landsman converter that uses fewer current sensors than the standard converter powers the BLDC. The cost and size of the motor drive system are greatly reduced as a result. To attain the most power possible from the PV system and achieve a voltage gain of 1:12 and efficiency of 97.42%, a modified P&O based MPPT method has been devised. Simulated analysis of the system confirms its efficacy. MATLAB Simulink model is used for simulating the entire system.

REFERENCES

[1] R. Kumar and B. Singh, "Single Stage Solar PV Fed Brushless DC Motor Driven Water Pump," in IEEE Journal of Emerging and Selected Topics in Power Electronics, vol. 5, no. 3, pp. 1377-1385, Sept. 2017, doi: 10.1109/JESTPE.2017.2699918.

[2] A. K. Mishra and B. Singh, "Solar Photovoltaic Array Dependent Dual Output Converter Based Water Pumping Using Switched Reluctance Motor Drive," in IEEE Transactions on Industry Applications, vol. 53, no. 6, pp. 5615-5623, Nov.-Dec. 2017, doi: 10.1109/TIA.2017.2732341.

[3] S. Murshid and B. Singh, "Analysis and Control of Weak Grid Interfaced Autonomous Solar Water Pumping System for Industrial and Commercial Applications," in IEEE Transactions on Industry Applications, vol. 55, no. 6, pp. 7207-7218, Nov.-Dec. 2019, doi: 10.1109/TIA.2019.2939705.

[4] S. Shukla and B. Singh, "Reduced Current Sensor Based Solar PV Fed Motion Sensorless Induction Motor Drive for Water Pumping," in IEEE Transactions on Industrial Informatics, vol. 15, no. 7, pp. 3973-3986, July 2019.

[5] M. Rezkallah, A. Chandra, M. Tremblay and H. Ibrahim, "Experimental Implementation of an APC With Enhanced MPPT for Standalone Solar Photovoltaic Based Water Pumping Station," in IEEE Transactions on Sustainable Energy, vol. 10, no. 1, pp. 181-191, Jan. 2019, doi: 10.1109/TSTE.2018.2829213.

[6] S. Murshid and B. Singh, "Implementation of PMSM Drive for a Solar Water Pumping System," in IEEE Transactions on Industry Applications, vol. 55, no. 5, pp. 4956-4964, Sept.-Oct. 2019, doi: 10.1109/TIA.2019.2924401.

[7] S. Murshid and B. Singh, "Single Stage Autonomous Solar Water Pumping System Using PMSM Drive," in IEEE Transactions on Industry Applications, vol. 56, no. 4, pp. 3985-3994, July-Aug. 2020, doi: 10.1109/TIA.2020.2988429.
[8] R. Antonello, M. Carraro, A. Costabeber, F. Tinazzi and M. Zigliotto, "Energy-Efficient Autonomous Solar Water-Pumping System for Permanent-Magnet Synchronous Motors," in IEEE Transactions on Industrial Electronics, vol. 64, no. 1, pp. 43-51, Jan. 2017, doi: 10.1109/TIE.2016.2595480.
[9] S. Murshid and B. Singh, "A Multiobjective GI-Based Control for Effective Operation of PV Pumping System Under Abnormal Grid Conditions," in IEEE Transactions on Industrial Informatics, vol. 16, no. 11, pp. 6880-6891, Nov. 2020, doi: 10.1109/TII.2019.2939838.
[10] A. K. Mishra and B. Singh, "High Gain Single Ended Primary Inductor Converter With Ripple Free Input Current for Solar Powered Water Pumping System Utilizing Cost-Effective Maximum Power Point Tracking Technique," in IEEE Transactions on Industry Applications, vol. 55, no. 6, pp. 6332-6343, Nov.-Dec. 2019, doi: 10.1109/TIA.2019.2929012.
[11] B. Singh, A. K. Mishra and R. Kumar, "Solar Powered Water Pumping System Employing Switched Reluctance Motor Drive," in IEEE Transactions on Industry Applications, vol. 52, no. 5, pp. 3949-3957, Sept.-Oct. 2016, doi: 10.1109/TIA.2016.2564945.
[12] R. Kumar and B. Singh, "BLDC Motor-Driven Solar PV Array-Fed Water Pumping System Employing Zeta Converter," in IEEE Transactions on Industry Applications, vol. 52, no. 3, pp. 2315-2322, May-June 2016, doi: 10.1109/TIA.2016.2522943.
[13] D. Venkatramanan and V. John, "Dynamic Modeling and Analysis of Buck Converter Based Solar PV Charge Controller for Improved MPPT Performance," in IEEE Transactions on Industry Applications, vol. 55, no. 6, pp. 6234-6246, Nov.-Dec. 2019, doi: 10.1109/TIA.2019.2937856.
[14] R. Kushwaha and B. Singh, "A Modified Luo Converter-Based Electric Vehicle Battery Charger With Power Quality Improvement," in IEEE Transactions on Transportation Electrification, vol. 5, no. 4, pp. 1087-1096, Dec. 2019, doi: 10.1109/TTE.2019.2952089.
[15] L. Callegaro, M. Ciobotaru, D. J. Pagano and J. E. Fletcher, "Feedback Linearization Control in Photovoltaic Module Integrated Converters," in IEEE Transactions on Power Electronics, vol. 34, no. 7, pp. 6876-6889, July 2019, doi: 10.1109/TPEL.2018.2872677.
[16] A. Mudlapur, V. V. Ramana, R. V. Damodaran, V. Balasubramanian and S. Mishra, "Effect of Partial Shading on PV Fed Induction Motor Water Pumping Systems," in IEEE Transactions on Energy Conversion, vol. 34, no. 1, pp. 530-539, March 2019.
[17] S. Shukla and B. Singh, "Reduced-Sensor-Based PV Array-Fed Direct Torque Control Induction Motor Drive for Water Pumping," in IEEE Transactions on Power Electronics, vol. 34, no. 6, pp. 5400-5415, June 2019.
[18] M. N. Ibrahim, H. Rezk, M. Al-Dhaifallah and P. Sergeant, "Solar Array Fed Synchronous Reluctance Motor Driven Water Pump: An Improved Performance Under Partial Shading Conditions," in IEEE Access, vol. 7, pp. 77100-77115, 2019.
[19] B. Singh and S. Murshid, "A Grid-Interactive Permanent-Magnet Synchronous Motor-Driven Solar Water-Pumping System," in IEEE Transactions on Industry Applications, vol. 54, no. 5, pp. 5549-5561, Sept.-Oct. 2018.
[20] K. K. Prabhakaran, A. Karthikeyan, S. Varsha, B. V. Perumal and S. Mishra, "Standalone Single Stage PV-Fed Reduced Switch Inverter Based PMSM for Water Pumping Application," in IEEE Transactions on Industry Applications, vol. 56, no. 6, pp. 6526-6535, Nov.-Dec. 2020.
[21] Javeed, Patan, Lochan Krishna Yadav, P. Venkatesh Kumar, Ranjit Kumar, and Shakti Swaroop, "SEPIC Converter for Low Power LED Applications," In Journal of Physics: vol. 1818, no. 1, p. 012220. IOP Publishing, 2021.
[22] Sivarajeswari, S., and D. Kirubakaran, "Design and development of efficient Luo converters for DC micro grid," The International Journal of Electrical Engineering &Education, pp. 0020720919845152, 2019.

